View metadata, citation and similar papers at core.ac.uk
brought to you by CORE
provided by Woods Hole Open Access Server

GEOPHYSICAL RESEARCH LETTERS, VOL. 31, L23311, doi:10.1029/2004GL021325, 2004

Seismic reflection imaging of water mass boundaries in the Norwegian Sea

Papia Nandi,[1] W. Steven Holbrook,[1] Scott Pearse,[2] Pedro Páramo,[1] and Raymond W. Schmitt[3]

Received 23 August 2004; revised 11 October 2004; accepted 3 November 2004; published 14 December 2004.

[1] Results from the first joint temperature and seismic reflection study of the ocean demonstrate that water mass boundaries can be acoustically mapped. Multichannel seismic profiles collected in the Norwegian Sea show reflections between the Norwegian Atlantic Current and Norwegian Sea Deep Water. The images were corroborated with a dense array of expendable bathythermographs and expendable conductivity-temperature depth profiles delineating sharp temperature gradients over vertical distances of ~5–15 m at depths over which reflections occur. Fine structure from both thermohaline intrusions and internal wave strains is imaged. Low-amplitude acoustic reflections correspond to temperature changes as small as 0.03°C implying that seismic reflection methods can image even weak fine structure. *INDEX TERMS:* 3025 Marine Geology and Geophysics: Marine seismics (0935); 4524 Oceanography: Physical: Fine structure and microstructure; 4283 Oceanography: General: Water masses. **Citation:** Nandi, P., W. S. Holbrook, S. Pearse, P. Páramo, and R. W. Schmitt (2004), Seismic reflection imaging of water mass boundaries in the Norwegian Sea, *Geophys. Res. Lett.*, *31*, L23311, doi:10.1029/2004GL021325.

1. Introduction

[2] The Earth's heat budget and climate system are strongly influenced by the ocean's thermohaline circulation [e.g., *Broecker*, 1997], in which water masses with distinct temperature/salinity characteristics distribute heat and water. Understanding the role of these water masses in large-scale thermohaline circulation requires the ability to map their positions and variability over time [*Fukasawa et al.*, 2004]. Boundaries between water masses are typically detected and mapped using temperature and salinity probes deployed at discrete locations or towed in a "tow-yo" fashion [*Rudnick and Ferrari*, 1999]. The interfaces between water masses often contain thermohaline fine structure [e.g., *Stommel and Federov*, 1967], or sharp changes in temperature and salinity over depth scales of several meters [*Gregg and Briscoe*, 1979] caused by dynamic processes such as vertical mixing [*Eckart*, 1948], intrusions from adjacent water masses [*Osborn*, 1998] or strains caused by internal gravity waves [*Garrett*, 1973]. Therefore, by employing remote techniques that detect fine structure it should be possible to map these boundaries. We present evidence that seismic reflection imaging can map water mass boundaries in great detail, with sensitivity to temperature fluctuations as small as 0.03°C.

[3] A recent study [*Holbrook et al.*, 2003] showed that seismic reflection methodology can image fine structure in a major oceanic front. Those authors speculated that deep acoustic reflections in the North Atlantic might correspond to a water mass boundary, but their study lacked corroborative measurements of temperature and salinity at those depths. The lack of temperature data in that study also made it difficult to quantify the sensitivity of the seismic reflection method to the magnitude of fine-scale temperature changes. Our study provides a detailed comparison of seismic reflectance and ocean temperature over a 172-km-long profile in the Norwegian Sea using a dense array of 33 expendable bathythermographs (XBTs) and 2 expendable conductivity-temperature depth (XCTDs) profiles. The resulting quantification of the sensitivity of the seismic reflection method to small changes in temperature implies applicability to a wider range of oceanographic processes than previously thought.

2. Methods

[4] The seismic data were acquired in September 2003 using the R/V *Maurice Ewing* in the Norwegian Sea. Acoustic energy was generated from 6 air guns with a volume of 1340 cubic inches (22 liters), fired every 37.5 m. A six-km-long streamer containing 480 hydrophone groups was towed behind the ship, resulting in a horizontal sampling spacing of 6.25 m. Reflected energy was sampled every 2 ms.

[5] Standard seismic processing steps, including velocity analysis, stacking, bandpass filtering and post-stack time migration were used to create the final seismic profile [*Yilmaz and Doherty*, 1987]. Fifteen to forty-fold stacking enhanced the signal-to-noise of water column reflections, typically much weaker than reflections from the seafloor. Water column reflections were migrated separately from subsurface geology to reduce migration artifacts.

[6] Thirty-five Sippican T-5 XBT and two XCTD-1 probes at an average horizontal spacing of 5 km were deployed during acquisition of the seismic reflection data. Ocean temperature was sampled by the XBT's approximately every 0.7 m, and temperature and salinity were sampled by the XCTD's every 0.1 m. The resulting temperature profiles were tied to the common midpoint nearest the XBT/XCTD deployment point in the combined seismic-temperature image.

3. Results and Discussion

[7] The Norwegian Sea, in our study area consists of warm Norwegian Atlantic Current (NwAC) and underlying

[1]Department of Geology and Geophysics, University of Wyoming, Laramie, Wyoming, USA.
[2]Department of Earth Sciences, University of Durham, Durham, UK.
[3]Department of Physical Oceanography, Woods Hole Oceanographic Institution, Woods Hole, Massachusetts, USA.

Copyright 2004 by the American Geophysical Union.
0094-8276/04/2004GL021325$05.00

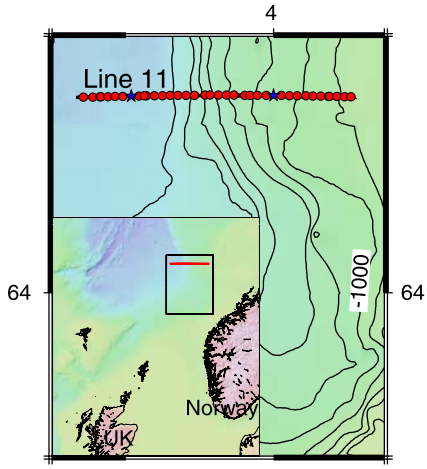

Figure 1. Bathymetric map of the study area in the Norwegian Sea. Line 11 is the seismic reflection survey, along which XBTs (red circles) and XCTDs (blue stars) were deployed. Inset shows the general location of the survey.

cold Norwegian Sea Deep Water (NSDW) (Figure 1). The NwAC, an extension of the North Atlantic Current flowing across the Iceland-Faeroe Ridge into the Norwegian Sea, has temperatures of 7–9°C and a salinity of ~35.2 psu [*Skagseth*, 2004; *Mauritzen*, 1996]. The NSDW, formed from mixing of Greenland Sea Deep Water and deep water from the Arctic Ocean, is colder (−0.5 to −1.1°C) and slightly less saline (34.92 psu) [*Swift*, 1986]. It is cooled by atmospheric heat loss in the Norwegian Sea and becomes denser, playing a key role in thermohaline circulation of the North Atlantic. Traditional sampling methods show the boundary between NwAC and NSDW at roughly 400 m depth [*Skagseth and Orvik*, 2002].

[8] A stacked seismic reflection profile on our transect shows a remarkable correlation to ocean temperature structure (Figure 2). Reflection patterns in the seismic image match water masses mapped by the XBT/XCTD survey: in the east, an upper, relatively non-reflective zone corresponds to the NwAC, which occupies the upper ~400 m, a lower non-reflective zone corresponds to the NSDW, which occupies ocean depths greater than ~600 m, and an intervening, strongly reflective zone corresponds to the boundary layer between the NwAC and the NSDW. Towards the west, the boundary layer shallows away from the continental margin and corresponds to reflections at ~200–400 m depth. Reflections generally follow isotherms, and, as will be discussed below, represent temperature fine structure in the boundary layer between the NwAC and NSDW. We can follow this fine structure laterally over the entire transect at a horizontal sampling interval of 6.25 m, observe its variability with depth and image internal waves occurring within it. The NwAC thins from 400 m near the continental slope to 200 m in the western part of the profile. Undulations representing small-scale internal waves occur in the boundary layer with amplitudes ranging from 9–13 m and wavelengths of 0.3–0.7 km.

[9] Detailed comparison of seismic reflections and temperature structure demonstrates that reflections mark the water mass boundary, which is rich in fine structure, on XBT and XCTD profiles. In the NwAC/NSDW boundary layer, reflectance matches fine-scale temperature variations, which have typical vertical distances of ~10 m between temperature gradient maxima (Figure 3). Interior portions of both the NwAC and the NSDW contain little fine structure in XBT data and are also largely acoustically transparent.

[10] Temperature fine structure is amenable to seismic imaging because fine structure occurs at vertical wavelengths comparable to those of typical marine reflection sound sources. Reflections are caused by acoustic impedance contrasts, which in this region are caused by abrupt vertical changes in temperature and thus sound speed. Our data contain reflections with a spectral content of 20–110 Hz and a dominant frequency of ~50 Hz. For an acoustic wave propagating through water at a velocity of 1480 m/s, the vertical resolution, or 1/4 wavelength [*Widess*, 1973], implies that individual layers as thin as about 4 m can be resolved.

[11] To better examine the relationship between fine structure and reflectance, we removed wavelengths greater than the dominant wavelength of the seismic source using a trapezoidal high-pass filter passing waves between 1/(35 m) and the Nyquist wavenumber from the temperature profiles (Figure 3). The remaining short-wavelength temperature fine structure matches reflections in the seismic image: positive and negative peaks in seismic amplitude correspond to sharp temperature increases and decreases, respectively, occurring over vertical distances of ~5–15 m in the XCTD profile. Fine structure revealed in the filtered XCTD contains temperature contrasts as great as 0.23°C, but most are smaller. The largest reflections, at 480 and 500 m, coincide with the largest changes in temperature. Several remarkably low-amplitude reflections correlate to small temperature changes between 700 and 800 m depth. The reflection at 770 m depth, for example, corresponds to a temperature contrast of 0.03°C (Figure 3). This surprising degree

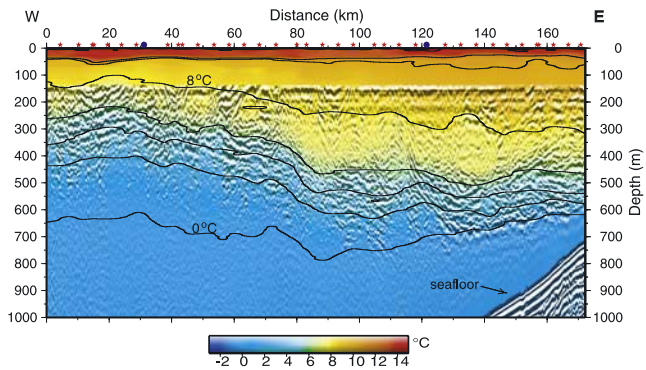

Figure 2. Ocean temperature (color) overlain by seismic reflection data (black). The warm (7–14°C) NwAC is separated from the cold (−0.5–2°C) NSDW by a boundary layer delineated by rapidly changing temperatures and clear seismic reflections. Thin solid lines are isotherms contoured every 2°C. Red stars and blue circles show locations of XBTs and XCTDs, respectively. The top 140 m of the seismic profile, containing interference from the direct arrival, has been muted, however reflectance from the bubble pulse is visible at ~160 and 215 m depth.

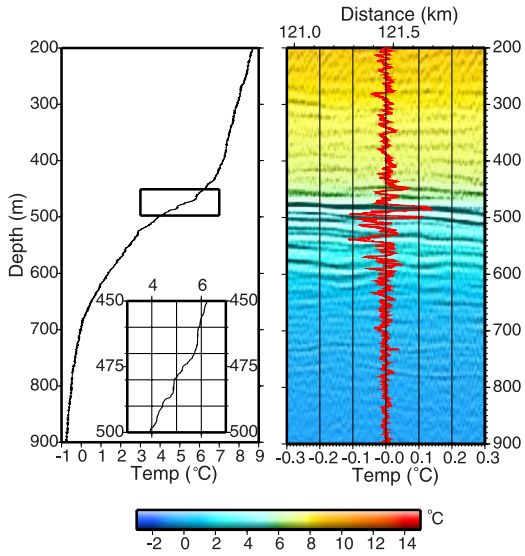

Figure 3. (a) An unfiltered XCTD profile located at km 121.5 on the seismic profile (Figure 2) showing temperature from 200–900 m depth. (b) Short-wavelength temperature variations (red), produced by removing wavelengths greater than 35 m from the XCTD temperature profile, plotted with a 5-km-wide section of the reflection image surrounding the XCTD location (black and white image). Background color scheme is ocean temperature, plotted as in Figure 2. The seismic image has been shifted upward by 14 m to reflect the lag between the onset of energy and peak amplitude in the seismic wavelet.

of sensitivity demonstrates that reflection seismology is capable of detecting even weak fine structure in the ocean.

[12] Close inspection of seismic amplitudes reveals a direct relationship to magnitudes of temperature contrasts. Reflection coefficients, a measure of impedance contrasts at reflection boundaries, were derived from the amplitudes of several prominent reflections. Reflection coefficients were calculated using the equation $R_i = A_i/A_0$ where A_i is the amplitude of the reflection, and $A_0 = -(A_{sf}^2)/A_{mult}$, where A_{sf} is the amplitude of the sea floor reflection, and A_{mult} is the amplitude of its first multiple [*Warner*, 1990]. In this XCTD, the largest temperature change of +0.22°C from 480 to 485 m corresponds to the largest positive reflection coefficient ($7.24 \times 10^{-4} \pm \sigma = 20\%$). Conversely, a smaller reflection coefficient ($1.43 \times 10^{-4} \pm \sigma = 43\%$) occurs at the smallest temperature change of +0.03°C. Similarly, other reflection coefficients have a positive correlation with temperature changes. Amplitudes are highest in the westernmost part of the profile, where filtered XBT data show average changes in temperature of +0.40°C. The easternmost part of the profile contains lower amplitude reflections coincident with smaller changes in temperature averaging +0.26°C, implying that amplitudes of seismic reflections are robust indicators of the relative magnitudes of temperature contrasts in the ocean.

[13] Comparison of seismic images with temperature and density data from XCTDs shows that temperature fine structure from internal wave strains and from density-compensated thermohaline intrusions [*Desaubies and Gregg*, 1981] has distinctive characteristics on the seismic sections. An XCTD taken from the eastern part of the profile (Figure 4a) shows variation of both temperature and density gradient occurring in lock-step, suggesting that these changes are caused by internal wave strains, which would change both density and temperature congruently. Reflections in this region are relatively weak and slope across several isotherms over 5 km, representing >2°C from a depth of ~540 m to ~450 m, clearly indicating the presence of an energy source away from the thermocline (Figure 4a). We interpret these as reflections from reversible fine structure caused by internal waves. This reversible fine structure is itself deformed by small-scale internal waves that deflect the sloping reflections into undulations with amplitudes of 5–13 m.

[14] In contrast, an XCTD profile taken from the western part of the line (Figure 4b) shows stronger temperature

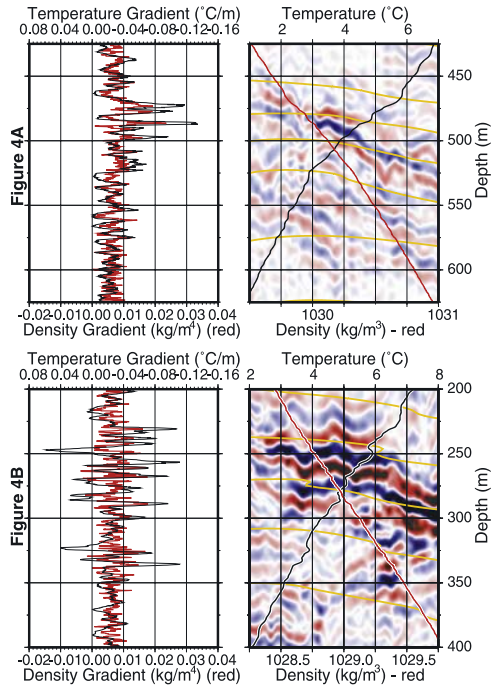

Figure 4. (a) (Left) Temperature and density gradient, calculated over a depth interval of 1 m from the XCTD profile located at km 121.5 on the seismic line. Temperature and density gradient vary concurrently, indicating internal wave strains. (Right) A 5-km-wide segment of seismic data centered at the XCTD (color), with temperature (black line) and density (red line) recorded by the XCTD. Isotherms of ocean temperature (yellow lines) are contoured at 1°C intervals. Internal waves appear in the seismic data as sloping reflections crossing isotherms. (b) (Left) Temperature and density gradient, plotted as in Figure 4a, at the XCTD profile located at km 31 on the seismic line. Density and temperature gradients do not co-vary at all depths, large fluctuations in temperature gradient at 250, 275 and 320 m are not matched by similar changes in density gradient. (Right) Temperature, density, seismic image and isotherms at the location of the XCTD, plotted in Figure 4a. A density-compensated temperature inversion at 250 m is coincident with bright reflections in the seismic profile. Reflections generally follow isotherms, deviating only by fractions of a degree as they are perturbed by small-scale internal waves.

gradients, including some positive temperature gradients corresponding to temperature inversions, and some variations in density gradient that do not vary together with temperature gradient. Large changes in temperature gradient at 250, 275 and 320 m occur in conjunction with little change in density stratification, indicating that salinity is compensating for changes in temperature and allowing for stirring along isopycnals. These observations are consistent with the presence of irreversible fine structure caused by thermohaline intrusions. Seismic reflections from the intrusions are stronger and more closely follow isotherms than reflections from internal wave strains (Figure 4b). These observations imply that, given temperature control from relatively inexpensive XBTs, seismic reflection images can provide information on the origin of fine structure and on the lateral and vertical extent over which the causative processes occur.

4. Conclusions

[15] The results of this study indicate that seismic reflection methodology can image the boundaries between water masses and record the lateral and vertical extent of the processes that form fine structure in the ocean. There is a clear correlation between seismic reflectance and thermohaline fine structure in XBT profiles. Specific reflectors can be correlated with intrusive fine structure, which often arises at the boundaries between water masses [*Lappo et al.*, 2001]. There is a direct relationship between reflection amplitudes and temperature contrasts, implying that future studies may be able to invert seismic reflection amplitudes to remotely estimate ocean temperature. The remarkable sensitivity of low-frequency reflection seismic imaging to temperature fine structure as small as 0.03°C implies that seismic imaging, with its very fine horizontal resolution and full depth capabilities, can provide new insights into the distribution of thermohaline intrusions, the presence of internal waves, and the morphology of deep water mass boundaries.

[16] **Acknowledgments.** We thank the crew of the *R/V Maurice Ewing* for a successful cruise, I. Fer, R. Ferrari, D. Shillington, P. Fulton, and J. Seymour for helpful conversations, and H. Brown and J. Nealon for data acquisition. Data were processed using Paradigm's Focus software and Generic Mapping Tools. Supported by NSF grants OCE-0221366 and OCE-0337289 to Holbrook.

References

Broecker, W. S. (1997), Thermohaline circulation, the Achilles heel of our climate system: Will man-made CO_2 upset the current balance?, *Science*, *278*, 1582–1588.

Desaubies, Y. J. F., and M. C. Gregg (1981), Reversible and irreversible fine structure, *J. Phys. Oceanogr.*, *11*, 541–556.

Eckart, C. (1948), An analysis of the stirring and mixing processes in incompressible fluids, *J. Mar. Res.*, *7*, 265–275.

Fukasawa, M., H. Freeland, R. Perkin, T. Watanabe, H. Uchidall, and A. Nishina (2004), Bottom water warming in the North Pacific Ocean, *Nature*, *427*, 825–827.

Garrett, C. (1973), The effect of internal wave strain on vertical spectira of fine-structure, *J. Phys. Oceanogr.*, *3*, 83–85.

Gregg, M. C., and M. G. Briscoe (1979), Internal waves, fine structure, microstructure and mixing in the ocean, *Rev. Geophys.*, *17*, 1524–1548.

Holbrook, W. S., P. Paramo, S. Pearse, and R. W. Schmitt (2003), Thermohaline fine structure in an oceanographic front from seismic reflection profiling, *Science*, *301*, 821–824.

Lappo, S. S., I. D. Lozovatsky, E. G. Morozov, A. V. Sokov, and S. M. Shapovalov (2001), Variability of water structure in the equatorial atlantic, *Dokl. Akad. Nauk Oceanol.*, *379A*, 739.

Mauritzen, C. (1996), Production of dense overflow waters feeding the North Atlantic across the Greenland-Scotland Ridge. Part 2: An inverse model, *Deep-Sea Res.*, *43*, 807–835.

Osborn, T. R. (1998), Finestructure, microstructure, and thin layers, *Oceanography*, *11*(1), 36–43.

Rudnick, D., and R. Ferrari (1999), Compensation of horizontal temperature and salinity gradients in the ocean mixed layer, *Science*, *283*, 526–529.

Skagseth, Ø. (2004), Monthly to annual variability of the Norwegian Atlantic slope current: Connection between the northern North Atlantic and the Norwegian Sea, *Deep-Sea Res. I*, *51*, 349–366.

Skagseth, Ø., and K. A. Orvik (2002), Identifying fluctuations in the Norwegian Atlantic Slope Current by means of Emperical Orthogonal Functions, *Cont. Shelf Res.*, *22*(4), 547–563.

Stommel, H., and K. N. Federov (1967), Small-scale structure in temperature and salinity near Timor and Mindanao, *Tellus*, *19*, 306–325.

Swift, J. H. (1986), The Arctic Waters, in *The Nordic Seas*, edited by B. G. Hurdle, pp. 129–153, Springer, New York.

Warner, M. (1990), Absolute reflection coefficients from deep seismic reflections, *Tectonophysics*, *173*, 15–23.

Widess, M. (1973), How thin is a thin bed?, *Geophysics*, *38*, 1176–1180.

Yilmaz, Ö., and S. Doherty (Eds.) (1987), *Seismic Data Processing*, *Invest. in Geophys.*, SEG, Tulsa, Ok.

W. S. Holbrook, P. Nandi, and P. Páramo, Department of Geology and Geophysics, University of Wyoming, Laramie, WY 82071, USA. (pnandi@uwyo.edu)

S. Pearse, Department of Earth Sciences, University of Durham, Durham DH1 3LE, UK.

R. W. Schmitt, Department of Physical Oceanography, Woods Hole Oceanographic Institution, Woods Hole, MA 02543, USA.